JOURNAL OF MASS SPECTROMETRY, VOL. 33, 144–153 (1998)

Gas-phase Acid–Base Chemistry and Its Effects on Mass Isotopomer Abundance Measurements of Biomolecular Ions

Clifton K. Fagerquist and Jean-Marc Schwarz*
Department of Nutritional Sciences and Toxicology, University of California, Berkeley, California 94720, USA

Various parameters which affect mass isotopomer abundance measurements of derivatives of palmitic acid ionized by electron ionization (EI) and electron-capture negative chemical ionization (ECNCI) were tested on a sector-field double-focusing mass spectrometer. Results on methyl palmitate ionized by EI are as follows: (i) sample size had a significant effect on mass isotopomer abundance ratios (MIARs); (ii) the electron multiplier gain of the detector also had an effect on MIARs; and (iii) ion scattering by ion–neutral collisions in the mass analyzer did not appear to have any significant effect on MIARs (under standard analysis conditions). However, 'reagent' gas pressure (methane) had a significant effect on MIARs of pentafluorylbenzyl palmitate ionized by ECNCI. It was concluded that there are two compensatory effects which alter MIARs of methyl palmitate ionized by EI: (i) gas-phase acid–base chemistry in the source (specifically, proton transfer between fragment cations and neutral molecules); and (ii) detector non-linearities, specifically, underestimation of less abundant isotopomers due to their signal disproportionately falling within the signal-to-noise ratio level of the electron multiplier. Gas-phase chemistry is the dominant cause of inaccuracy in MIAR measurements for large sample sizes, while detector non-linearity is the dominant cause of inaccuracy in MIAR measurements at small sample sizes. However, in a narrow intermediate range of sample size, these two effects balance each other and result in MIARs which are 'acceptable' when compared with the known MIAR values. It is emphasized that these two effects are present regardless of the type of mass analyzer used, e.g. quadrupole, sector-field. Improvements in the accuracy of MIAR measurements will require developments in mass spectrometry aimed at eliminating each of the contributory effects. © **1998 John Wiley & Sons, Ltd.**

J. Mass Spectrom. **33**, 144–153 (1998)

KEYWORDS: proton transfer; hydride ion abstraction; self-chemical ionization; mass isotopomer distribution analysis

INTRODUCTION

Extraction of quantitative information from isotopic abundance ratios of atoms or simple molecules is a small but growing field in mass spectrometry. Techniques such as gas chromatography/isotope ratio mass spectrometry (GC/IRMS) and inductively coupled plasma mass spectrometry (ICP-MS), require the combustion/destruction of the sample followed by isotopic analysis of the products, usually atoms or small molecules.[1–3] A relatively new and technically challenging application in isotopic abundance measurements is the extraction of quantitative information from the isotopomer abundances of *intact* biomolecular ions, such as fatty acids, glucose, cholesterol and peptides. Samples of these biomolecules are obtained from subjects who have been infused with a stable-isotope labeled precursor. Statistical analysis of the isotopomer pattern allows calculation of *in vivo* biosynthetic rates and precursor pool enrichments. Such information is of extreme usefulness in the fields of physiology and medicine.[4–7] However, the difficulties of accurate and precise isotopomer abundance measurements, of even small biomolecules, are formidable.

Errors in such measurements may originate from chemical, physical or instrumental causes. A number of explanations have been put forward for the causes of inaccuracies, including gas-phase chemistry in the source, peak broadening due to ion scattering in the mass analyzer and detector non-linearities. Tulloch and Hogge[8] first noted a sample size effect on the isotopomer abundances of molecular ions of fatty acid methyl esters (FAMES) analyzed by GC/electron impact (EI) MS. They proposed that proton transfer between a *rearranged* molecular ion and a neutral molecule was the most likely cause of the increase in the less abundant isotopomers as a function of the amount of sample injected into the source. The possibility of fragment ions also contributing to proton transfer was also speculated.[8] In subsequent work, Patterson and Wolfe[9] studied methyl palmitate by GC/EI-MS and

* *Correspondence to:* J.-M. Schwarz, Department of Nutritional Sciences and Toxicology, University of California, Berkeley, California 94720, USA
E-mail: jschwarz@nature.berkeley.edu

CCC 1076–5174/98/020144–10 $17.50

Received 9 September 1997
Accepted 5 November 1997

observed a similar sample concentration dependence. They noted that the concentration dependence was second order and proposed that gas-phase hydrogen abstraction was the dominant cause of the observed effect. They also emphasized the consequences of the concentration dependence for tracer methodology studies and proposed a *post-hoc* mathematical correction. Two other possible explanations, i.e. detector non-linearity and ion scattering caused by ion–ion repulsions or ion–neutral collisions, were discounted as not being significant contributors to the concentration dependence. Detector non-linearity was ruled out because of the lack of an effect as a function of the electron multiplier voltage. Ion–neutral collisions and/or ion–ion repulsions were ruled out because of the absence of a 'concentration' effect for a *tert*-butyldimethylsilyl derivative of urea over a similar sample size and ion current range which suggested that the chemical composition of the sample was responsible for the concentration dependence.[9]

Kienle and Magni[10] observed a similar concentration dependence for methyl palmitate on a GC/MS quadrupole instrument (Finnigan 4021) but not on a magnetic sector instrument (LKB 2091). They concluded that the concentration effect was unique to quadrupole instruments, perhaps owing to the type of source or source parameters. They agreed with Patterson and Wolfe[9] that gas-phase hydrogen abstraction was the likely cause of the concentration effect, and suggested that since the concentration effect was limited to the molecular ion, alternative analysis of a fragment ion (which still contained the relevant isotopic information) might eliminate the observed concentration dependence even on quadrupoles. Following up on Kienle and Magni's suggestion, Zamecnik *et al.*[11] tested a pentafluorylbenzyl derivative of palmitic acid on a quadrupole GC/MS instrument (Hewlett–Packard 5970). The carboxylate cation of palmitic acid was analyzed by selected-ion monitoring and found to have significantly less concentration dependence than analysis of the molecular ion. In addition, Zamecnik *et al.*[11] pointed out that *protonation* (via self-CI) was the more likely cause of the concentration effect.

Peak broadening caused by ion scattering (due to ion–ion repulsions or ion–neutral collisions in the mass analyzer) has been known for many years by researchers measuring isotopic abundances of atoms and simple molecules.[12] The phenomenon, generally referred to as abundance sensitivity, is primarily a result of ion–neutral collisions in the mass analyzer causing peak broadening and overlap of adjacent isotopic peaks. Isotopomer overlap results in the most abundant isotopomer being underestimated and the less abundant isotopomers being overestimated.

Bergner and Lee[13] proposed that detector non-linearity was responsible for a significant concentration effect. Comparative measurements were made which revealed response differences between two types of amplifying circuit boards: linear and non-linear. The non-linear amplifying circuit board gave a much more severe concentration effect as a function of the total ion current (TIC).[13]

We decided to pursue our own investigations of this problem(s) and assess the likely cause(s) of inaccuracies in isotopomer measurements using a recently acquired sector-field mass spectrometer. In this paper, we report our results for measurements of methyl palmitate ionized by EI and pentafluorylbenzyl palmitate ionized by electron-capture negative chemical ionization (ECNCI).

EXPERIMENTAL

The instrument used for these measurements was a JEOL (Peabody, MA, USA) AX505 double-focusing mass spectrometer. It is a 'forward' geometry E/B sector-field instrument (S-configuration). Methyl palmitate was ionized by EI at 70 eV and pentafluorylbenzyl palmitate by ECNCI using methane as the 'reagent' gas. Samples were introduced into the mass spectrometer via a gas chromatograph (Hewlett–Packard 6890) using a DB-5 30 m × 0.32 mm i.d. capillary column (J&W Scientific). The initial GC oven temperature was 100 °C followed by a 20 °C/min ramp to a final temperature of 250 °C. The source temperature was 230 °C. Typical sample concentrations were 100 ng μl^{-1} with 0.5–2.5 μl injections.

Ions were accelerated out of the source at 3.0 kV, after which they passed through the toroidal electrostatic plates of the electric sector. An octopole lens focused the ions from the electric to the magnetic sector. Ions were deflected toward an off-axis conversion dynode at a voltage of −10.0 kV. The secondary electrons emitted from the conversion dynode by ion impact were amplified by a 16-dynode cascade electron multiplier (Hamamatsu Photonics). With the exception of testing the effect of the electron multiplier, all measurements were performed at an electron multiplier voltage of 1.0 kV.

Mass isotopomer abundance measurements were performed using selected ion-monitoring/electric-field jumping (SIM/EFJ). The switching rate was 50 ms. Prior to every SIM measurement a separate magnetic and electric field calibration was performed using perfluorokerosene as calibrant. A final peak adjust calibration was performed using the sample molecule as calibrant introduced through the gas chromatograph. The final peak adjust calibration insured that the SIM measurement was centered on the maxima of each isotopomer. Only the three most abundant isotopomers of the parent ion (or a fragment ion which retains the isotopic information of interest) were monitored. Instrument performance was tested with natural abundance standards.

Source pressure was monitored by a Penning ion gauge located above a 6 in diffusion pump of the source chamber. However, the actual pressure in the ionization housing and along the ion beam path toward the exit slit is likely to be higher during sample introduction from the GC capillary. The mass analyzer pressure was measured by a Penning ion gauge located above the gate valve of a 3 in diffusion pump which was attached by a 90° elbow to the mass analyzer at the electric sector. Under normal operation the analyzer pressure was 1×10^{-7}–1×10^{-6} Torr (1 Torr = 133.3 Pa). However, the analogue meter had a lower limit of

1×10^{-6} Torr, which was considered the upper pressure limit during normal operation.

DATA ANALYSIS

We refer to the isotopomer with the lowest m/z as $I_{m=0}$, the next highest m/z ion as $I_{m=1}$ and the isotopomer with the highest m/z as $I_{m=2}$. Normalized abundances are designated M_0, M_1 and M_2, where $M_0 = I_{m=0}/\sum_{m=0-2} I_m$, $M_1 = I_{m=1}/\sum_{m=0-2} I_m$ and $M_2 = I_{m=2}/\sum_{m=0-2} I_m$. Every data point is the average of three consecutive injections with error bars showing the standard deviation. M_0, M_1 and M_2 will be collectively referred to as the mass isotopomer abundance ratios (MIARs) and $\sum_{m=0-2} I_m$ as the total isotopomer ion abundance (TIIA).

RESULTS

Electron impact ionization of methyl palmitate

Sample size. Figure 1 shows the change in the three most abundant isotopomers of methyl palmitate as a function of the amount of sample injected into the source. We observed a typical concentration dependence, i.e. M_0 declined and M_1 and M_2 increased as the amount of material injected into the source increased. The y-intercepts and slopes varied somewhat from day-to-day, but the decrease in M_0 and increase in M_1 and M_2 as a function of increasing sample size remained constant. Note that at low concentration M_0 is above and M_1 and M_2 are below their natural abundance values.

Second-order sample size dependence. We have taken our $I_{m=0}$ and $I_{m=1}$ data plotted in Fig. 1 and replotted them in Fig. 2 to see if we observed a second-order sample size dependence previously noted by Patterson and Wolfe[9] on a quadrupole mass spectrometer. $I_{m=1}$ *vs.* $I_{m=0}$ (bottom panel) and $I_{m=1}/I_{m=0}$ *vs.* $I_{m=0}$ (top panel) are plotted in Fig. 2. For $I_{m=1}$ *vs.* $I_{m=0}$ linear (dashed line) and second-order (solid line) regressions were plotted from the data. A better fit was obtained using a second-order polynomial, although we obtained a non-zero y-intercept: $y = 0.018\,33 + 0.190\,70\,x + 1.372\,23 \times 10^{-5}\,x^2$. For $I_{m=1}/I_{m=0}$ *vs.* $I_{m=0}$ a linear regression is plotted: $y = 0.190\,92 + 1.350\,76 \times 10^{-5}\,x$. It is interesting that our $I_{m=1}/I_{m=0}$ *vs.* $I_{m=0}$ plot gives a y-intercept of 0.190 92, which is significantly closer to the correct natural abundance value of 0.1934 compared with the value reported by Patterson and Wolfe[9] of ~0.183. However, this may reflect differences in detector response of the two instruments.

Our $I_{m=1}$ and $I_{m=2}$ data plotted in Fig. 1 are replotted as $I_{m=2}$ *vs.* $I_{m=1}$ (bottom panel) and $I_{m=2}/I_{m=1}$ *vs.* $I_{m=1}$ (top panel) in Fig. 3. Again, a better fit was obtained for $I_{m=2}$ *vs.* $I_{m=1}$ using a second-order polynomial regression, although we still obtain a non-zero

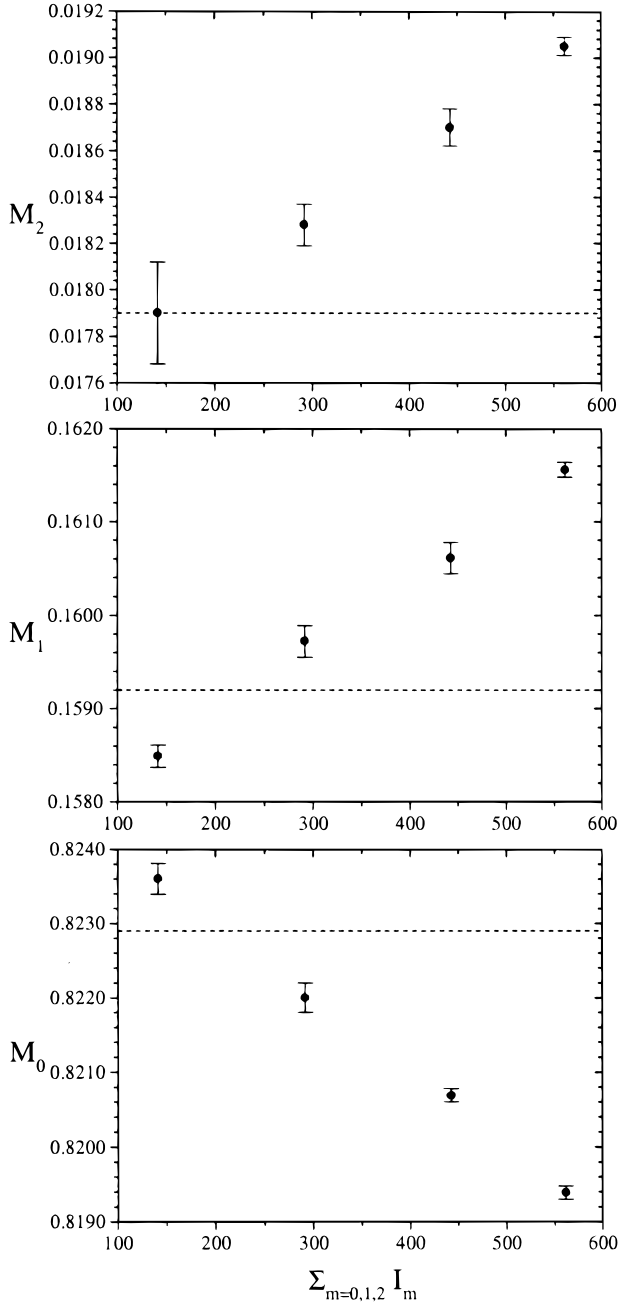

Figure 1. Change in the abundances of the three most abundant isotopomers of methyl palmitate, M_0, M_1 and M_2, as a function of injected sample size (0.5, 1.0, 1.5 and 2.0 μl) reflected in the total isotopomer intensity ($\sum_{m=0-2} I_m$). Each data point represents the average of three consecutive injections. Error bars represent the standard deviation. The dashed line is the normalized natural abundance of the isotopomer.

y-intercept: $y = 0.016\,49 + 0.110\,37\,x + 8.112\,61 \times 10^{-5}\,x^2$. It is interesting that the second-order coefficient is greater for $I_{m=2}$ *vs.* $I_{m=1}$ than $I_{m=1}$ *vs.* $I_{m=0}$, which may reflect the differences in abundances of $I_{m=2}$ *vs.* $I_{m=1}$ (0.0179 *vs.* 0.1592) compared with $I_{m=1}$ *vs.* $I_{m=0}$ (0.1592 *vs.* 0.8229).

Electron multiplier voltage. Figure 4 shows the change in the three most abundant isotopomers of methyl palmitate as a function of sample size and electron multiplier voltage. Along with the previously noted sample-size

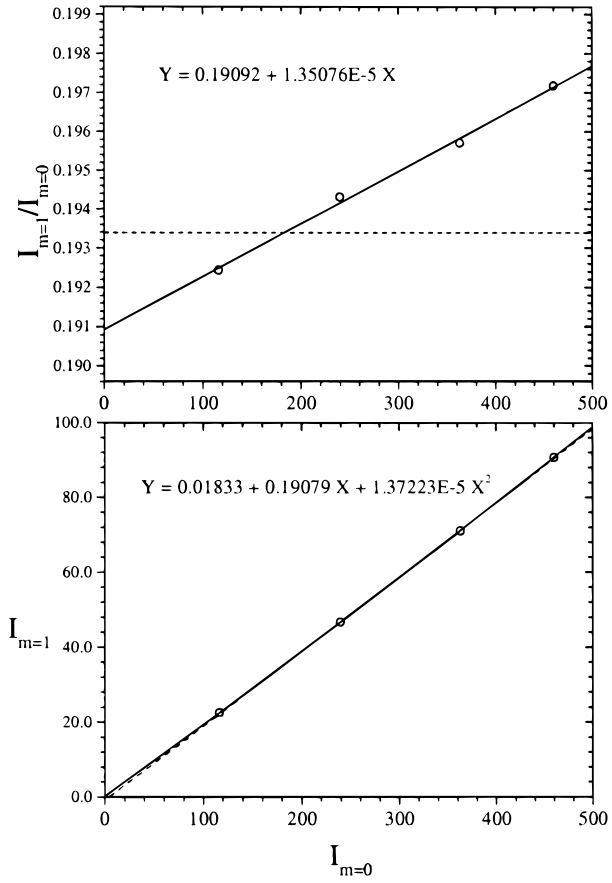

Figure 2. Second-order sample-size dependence. Integrated peak areas of I_{m-0} and I_{m-1} taken from data displayed in Fig. 1. Bottom panel: I_{m-1} *vs.* I_{m-0}. Linear (dashed line) and second-order (solid line) regressions are plotted from the data. A better fit was obtained with a second-order dependence. The equation for second-order dependence is shown. Top panel: I_{m-1}/I_{m-0} *vs.* I_{m-0}. Linear regression plotted and equation shown. The dashed line is the natural abundance ratio: I_{m-1}/I_{m-0}.

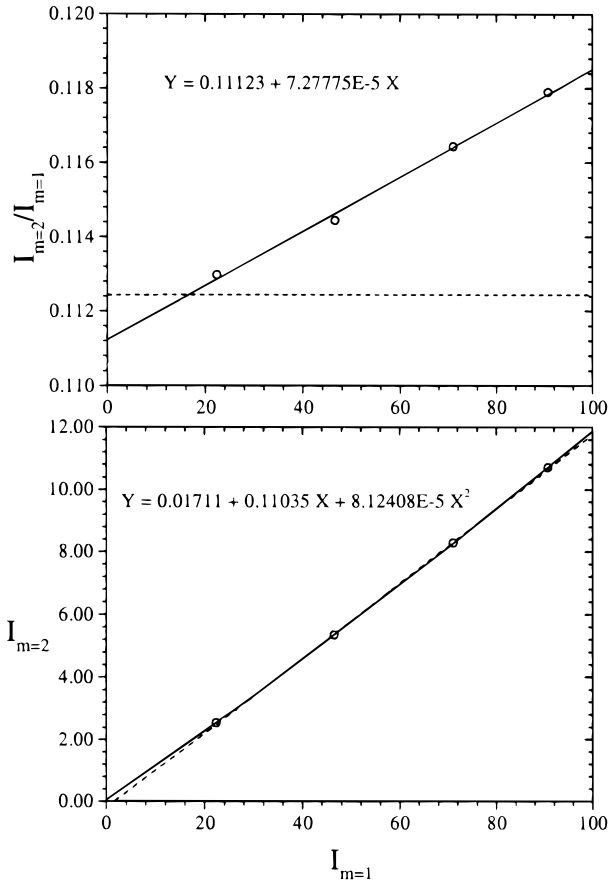

Figure 3. Second-order sample-size dependence. Integrated peak areas of I_{m-1} and I_{m-2} taken from data displayed in Fig. 1. Bottom panel: I_{m-2} *vs.* I_{m-1}. Linear (dashed line) and second-order (solid line) regressions are plotted from the data. A better fit was obtained with a second-order dependence. The equation for second-order dependence is shown. Top panel: I_{m-2}/I_{m-1} *vs.* I_{m-1}. Linear regression plotted and equation shown. The dashed line is the natural abundance ratio: I_{m-2}/I_{m-1}.

effect, we observed a change in the MIARs and TIIA as a function of electron multiplier voltage. M_2 was found to increase at the higher electron multiplier voltage for all sample sizes, whereas M_0 and M_1 decreased (or remained roughly unchanged).

Ionization current, sample size and TIIA. Table 1 shows the change in the three most abundant isotopomers of methyl palmitate as a function of sample size and ionization current. Compensatory variation of sample size and ionization current resulted in roughly constant TIIA.

Since ion–molecule collisions are required for any gas-phase ion–molecule chemistry, we tested the effect of increasing the number of ion–molecule collisions while keeping TIIA constant. This was accomplished by compensatory variation of ionization current, i.e. the number of ionizing electrons, and sample size, i.e. the number density of sample molecules. The AX505 has two ionization current settings, 100 or 300 μA. It was therefore possible to inject a full sample size when ionizing at 100 μA followed by one-third the sample size ionizing at 300 μA and obtain roughly the same TIIA for both injections. The MIARs show a decline in M_0 and increase in M_1 and M_2 when comparing the smaller with the larger sample size. One would expect a greater number of ion–molecule collisions for the larger sample size injected, because of the greater number density of molecules in the source. In consequence, more ion–molecule collisions result in more ion–molecule chemistry which alters the MIARs.

Table 1. Sample Size, Ionization Current and Isotopomer Abundances

Sample (μl)	Current (μA)	TIIA	M_0	M_1	M_2
0.5	300	950.7 ± 33.5	0.825 29 ± 0.000 29	0.156 66 ± 0.000 24	0.018 05 ± 0.000 06
1.5	100	1073.8 ± 4.8	0.824 04 ± 0.000 02	0.157 61 ± 0.000 06	0.018 35 ± 0.000 006

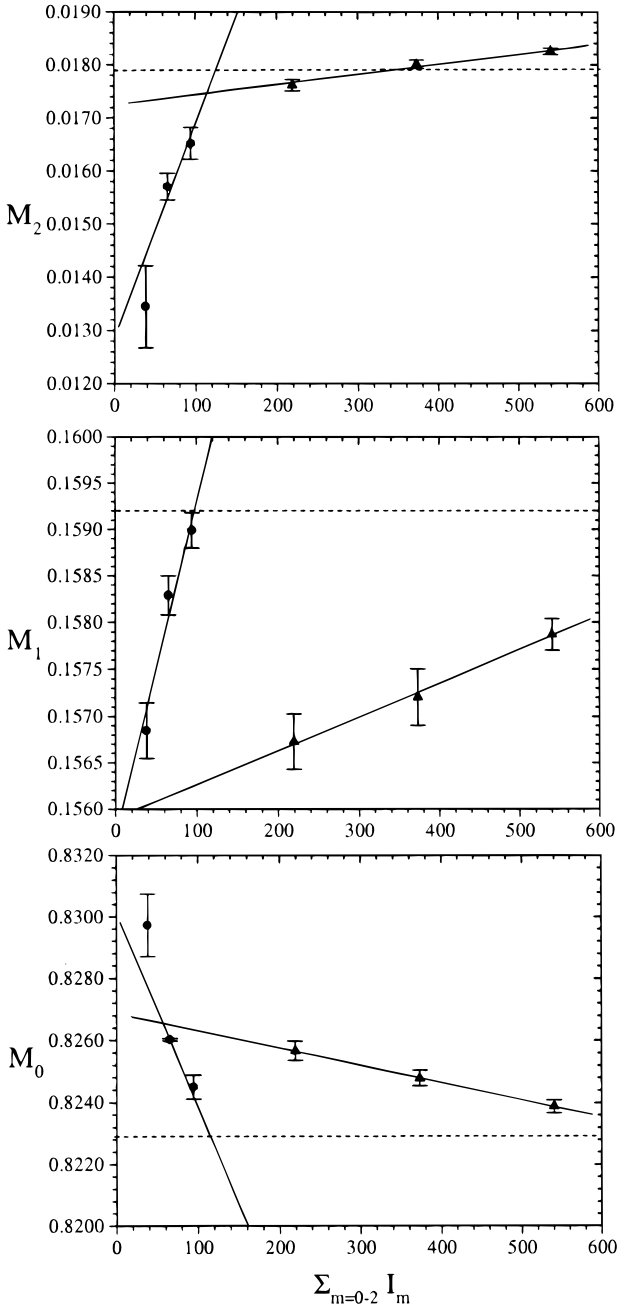

Figure 4. Change in the abundances of the three most abundant isotopomers of methyl palmitate, M_0, M_1 and M_2, as a function of injected sample size (0.5, 1.0 and 1.5 µl) and electron multiplier voltage (1.0 and 1.2 kV) as reflected in the total isotopomer integrated peak areas ($\sum_{m=0-2} I_m$). Each data point represents the average of three consecutive injections. Error bars represent the standard deviation. Solid circles are data collected at a multiplier voltage of 1.0 kV. Solid triangles are data collected at a multiplier voltage of 1.2 kV. Best-fit lines are drawn through the data which have the same electron multiplier voltage. The dashed line is the normalized natural abundance of the isotopomer.

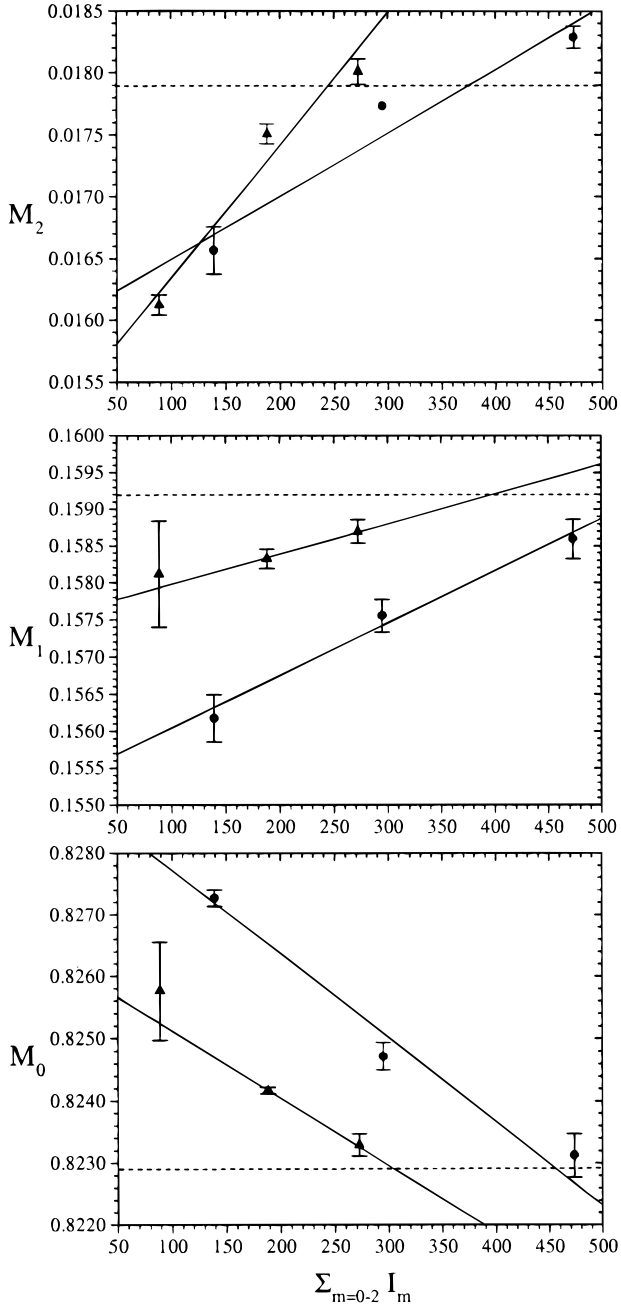

Figure 5. Change in the abundances of the three most abundant isotopomers of methyl palmitate, M_0, M_1 and M_2, as a function of injected sample size (0.5, 1.0 and 1.5 µl) and carrier gas pressure (7×10^{-6} and 1.5×10^{-5} Torr) as reflected in the total isotopomer integrated peak areas ($\sum_{m=0-2} I_m$). Each data point represents the average of three consecutive injections. Error bars represent the standard deviation. Solid circles are data collected at a source pressure of 7×10^{-6} Torr. Solid triangles are data collected at a source pressure of 1.5×10^{-5} Torr. Best-fit lines are drawn through the data which have identical source pressure. The dashed line is the normalized natural abundance of the isotopomer.

Carrier gas pressure. Figure 5 shows the change in the three most abundant isotopomers as a function of sample size and carrier gas (argon) pressure. Measurements were taken at two different carrier gas pressures, 7×10^{-6} and 1.5×10^{-5} Torr (as measured by the Penning ion gauge of the source). TIIA was reduced at the higher pressure, undoubtedly due to the neutral species being swept from the source faster than at the lower pressure.

Electron-capture negative chemical ionization (ECNCI) of pentafluorylbenzyl palmitate

Reagent gas pressure. Figure 6 shows the change in the three most abundant isotopomers of the carboxylate anion of palmitic acid as a function of sample size and reagent gas pressure (methane). Measurements were taken at two different reagent gas pressures, 1.5×10^{-5} and 2.5×10^{-5} Torr (as measured by the Penning ion gauge of the source).

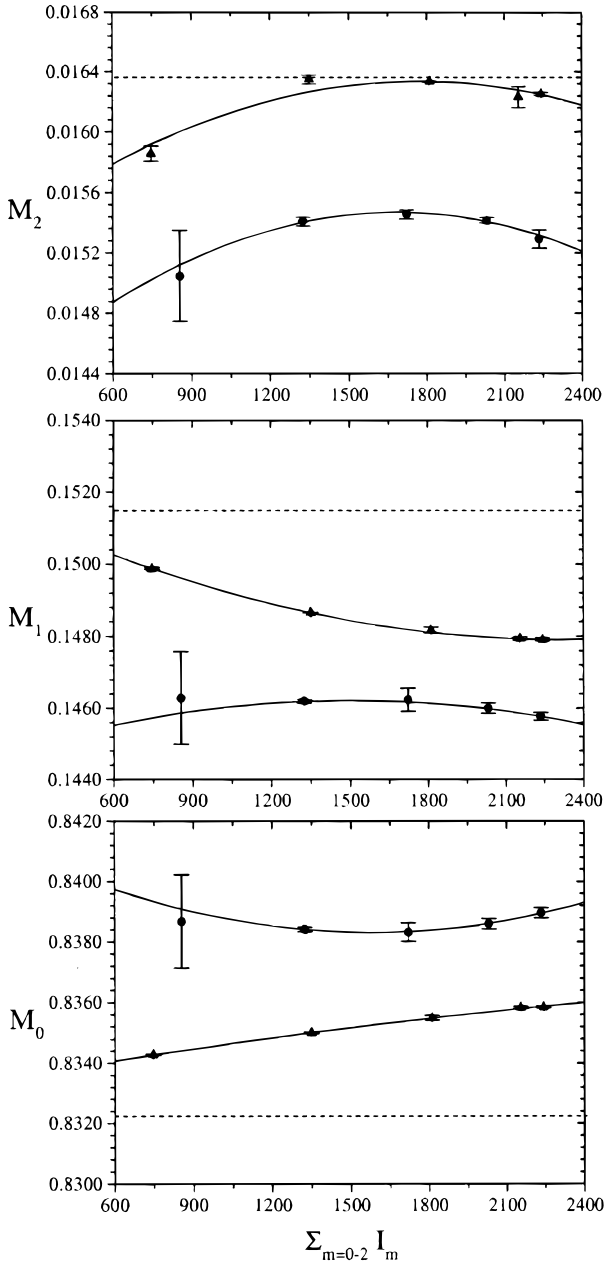

Figure 6. Change in the abundances of the three most abundant isotopomers of the carboxylate anion of palmitic acid, M_0, M_1 and M_2, as a function of injected sample size (0.5, 1.0, 1.5, 2.0, 2.5 μl) and reagent gas pressure (1.5×10^{-5} and 2.5×10^{-5} Torr) as reflected in the total isotopomer integrated peak areas ($\sum_{m=0-2} I_m$). Each data point represents the average of three consecutive injections. Error bars represent the standard deviation. Solid circles are data collected at a source pressure of 1.5×10^{-5} Torr. Solid triangles are data collected at a source pressure of 2.5×10^{-5} Torr. Best-fit lines are drawn through data points having the same source pressure. The dashed line is the normalized natural abundance of the isotopomer.

DISCUSSION

The source

Gas-phase acid–base chemistry. From our results and those of previous researchers, it is apparent that gas-phase ion–molecule chemistry plays a significant role in MIARs of fatty acid methyl esters (FAMES).[8,9] The reaction mechanism has been variously postulated with the two most likely candidates being hydrogen abstraction[9] and proton transfer.[8,11] These two reaction mechanisms, although similar, are still distinctly different. We feel that this subject, although well documented, deserves review and may help to emphasize inherent problems in MIARs measurements of biomolecular ions in general and FAMES in particular.

Hydrogen abstraction is the removal of a hydrogen atom from a neutral molecule to a cation. There is no transfer of charge for this reaction mechanism. Thus, hydrogen abstraction from $m_0{}^0$ to $m_0{}^+$ gives m^+_{0+H}, which is indistinguishable from $m_1{}^+$ at resolutions of $m/\Delta m < 100\,000$. Hydrogen abstraction from $m_0{}^0$ to $m_1{}^+$ gives m^+_{1+H}, which is indistinguishable from $m_2{}^+$, and so forth. Hydrogen removal is most likely to occur from the long alkyl chain of the neutral to the ionized carbonyl oxygen of the cation. Multiple ion–molecule collisions could also result in multiple hydrogen additions to the ionized carbonyl oxygen.

In contrast to hydrogen abstraction, proton transfer involves the transfer of both mass *and* charge. Proton exchange is more likely to occur between a fragment ion and a neutral molecule than between a molecular ion and neutral molecule owing to the greater abundance of fragment ions when ionizing by EI as well as a favorable thermochemistry (to be discussed later). Figure 7 shows a full scan spectrum of methyl palmitate on the AX505. It reveals the characteristic fragmentation pattern observed for FAMES ionized by EI. The most abundant ion at *m/z* 74 is generated by the exhaustively studied McLafferty rearrangement.[14,15] The McLafferty rearrangement (McLR) is the formation of a hexacyclic transition state from the carbonyl oxygen, the carbonyl carbon C-1, C-2, C-3 and C-4 and one of the C-4 hydrogens. Formation of this transition state is followed by intramolecular hydrogen transfer of a C-4 hydrogen to the carbonyl oxygen. Bond cleavage then occurs between the C-2 and C-3 resulting in a fragment ion with *m/z* 74. The second most abundant ion is at *m/z* 87 which is generated by a similar rearrangement followed by hydrogen transfer from the C-5, C-6 or C-7 carbons to the carbonyl oxygen with subsequent fragmentation between the C-3 and C-4 carbons. The initial rearrangement occurs on a time-scale of 10^{-10} s with the rates of subsequent steps dependent upon the internal energy of the ion. The time-scale for the generation of *m/z* 74 or 87 ions is less than the source residence time of 10^{-6}–10^{-7} s based on recent observations which have shown that metastable molecular ions which undergo dissociation after leaving the source do not generate the fragment ions at *m/z* 74 or 87.[16–18] Since *m/z* 74 and 87 are positively charged fragment ions, the hydrogen bound to the carbonyl oxygen is acidic. A collision between the *m/z* 74 or 87 ion (or other fragment ions shown in Fig. 7) with a sample molecule can result in proton transfer to the carbonyl oxygen of the neutral. Thus, proton transfer to $m_0{}^0$ gives m^+_{0+H}, which is instrumentally indistinguishable from $m_1{}^+$. Proton transfer to $m_1{}^0$ gives m^+_{1+H}, which is indistinguishable from $m_2{}^+$, and so forth.

Another gas-phase reaction mechanism which involves transfer of both mass and charge is hydride ion

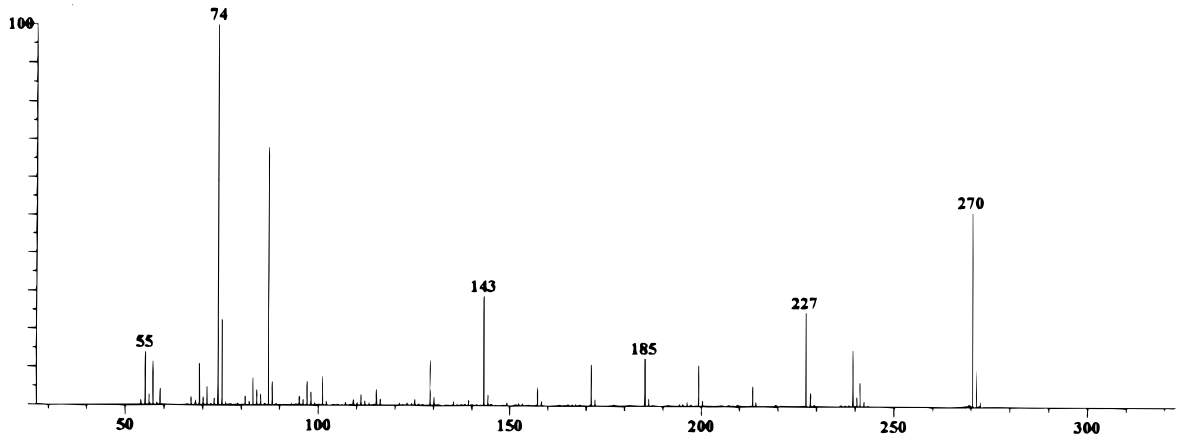

Figure 7. Full-scan spectrum of methyl palmitate ionized by EI (70 eV).

abstraction. Hydride ion abstraction is the removal of an H^- from a neutral molecule to a cation. Hydride ion abstraction from $m_0{}^0$ would give m^+_{0-H} or m^+_{-1}. Hydride ion abstraction from $m_1{}^0$ neutral would give m^+_{1-H}, which is indistinguishable from $m_0{}^+$, and so on. Hydride ion abstraction (like hydrogen abstraction) is most likely to occur at the long alkyl chain of a FAME.

Proton transfer and hydride ion abstraction are both mechanisms which are determined by the gas-phase acidity (GA) of the reactant ion and the gas-phase basicity (GB) of the reactant molecule (proton donation is a Brønsted–Lowry acid mechanism, whereas hydride ion abstraction is a Lewis acid mechanism). For example, studies on methyl stearate ($M_r = 298$) with positive CI (methane or hydrogen) showed almost equal ion abundances of *m/z* 299 (proton transfer) and *m/z* 297 (hydride ion abstraction), suggesting that the amount of proton transfer to and hydride ion abstraction from methyl stearate were almost equivalent.[19] This is a reflection of the large hydride ion affinities of the reactant ions of $CI_{hydrogen}$ and $CI_{methane}$: 300 kcal mol^{-1} for $H_3{}^+$ and 269 and 271 kcal mol^{-1} for $CH_5{}^+$ and $C_2H_5{}^+$, respectively (1 kcal = 4.184 kJ).[20] The fact that the amount of hydride ion abstraction was found to increase with increasing alkyl chain length was due to the greater the number of hydride ions for potential abstraction. Which mechanism dominates for the McLR ions at *m/z* 74 and 87 (and also other fragment ions shown in Fig. 7) would depend on their GAs. These values are not currently available; however, the favorability of proton donation from or hydride ion abstraction to *m/z* 74 and 87 ions with a methyl palmitate molecule can be estimated from the values given in Table 2.

For instance, if we assume that the proton affinity (*PA*) of CH_2COOCH_3 ($M_r = 73$) is roughly the same as that of CH_3COOCH_3 (methyl acetate)—a not unreasonable assumption—then proton donation from $CH_2COH^+OCH_3$ (*m/z* 74) to a methyl palmitate molecule is exothermic by $\sim$5 kcal mol^{-1} (0.25 eV). Munson and co-workers[21] have shown that the *PA*s of FAMES increase with increasing alkyl chain length. Hence any fragment ions (retaining the carboxyl group) which have alkyl chains shorter than the molecular ion, such as *m/z* 74, 87, 101, 127, 143, 185, 199 and 227, will probably have a neutral *PA less* than that of the methyl palmitate molecule. In consequence, proton transfer *from* the fragment cation *to* the neutral molecule is exothermic by a few kcal mol^{-1}.

The favorability of hydride ion abstraction from a methyl palmitate molecule to fragment ions *m/z* 74 and 87 can be estimated if we assume that the hydride ion affinity (*HIA*) of fragment cations *m/z* 74 or 87 are roughly comparable to that of $(Me_2)C{=}OH^+$ and the *HIA* of $CH_3CH_2CH^+CH_3$ is comparable to that of the alkyl chain of methyl palmitate. Using these assumptions, hydride ion abstraction from a methyl palmitate alkyl chain to fragment cations *m/z* 74 or 87 is endothermic by $\sim$ +30 kcal mol^{-1} (+1.3 eV). These rough comparisons suggest that hydride ion abstraction is endothermic. However, hydride ion abstraction may still occur to some extent because the neutral molecules are often highly vibrationally excited. Hence their internal energy may assist in overcoming the endothermicity of this mechanism. In addition, there would be many more ion–alkyl chain collisions than ion–carboxyl group collisions, because the cation is more likely to collide with the long alkyl chain than with the carboxyl group of the neutral. However, ion–dipole interactions should, to some extent, orient the electron-rich carboxyl group of the neutral toward an approaching cation prior to collision.

Further evidence supporting gas-phase acid–base chemistry affecting MIARs comes from previous work by Tulloch and Hogge,[8] who, in addition to studying the effect of sample size on isotopomer abundances, also examined the effect of alkyl chain length on fragmentation and MIARs for a series of FAMES. They observed

Table 2. Thermochemistry

Proton affinities: H^+ (PA) (kcal mol^{-1})	
Methyl palmitate	202.75 ± 0.25[21]
CH_3COOCH_3	198.3[22] (197.9[23])
CH_2COOCH_3 ($M_r = 73$)	NA
$CH_3CH_2COOCH_3$	200.3[23]
$CH_2CHCOOCH_3$ ($M_r = 86$)	NA
Hydride Ion Affinities: H^- (HIA)[22] (kcal mol^{-1})	
$CH_3CH_2CH^+CH_3$	247
$(CH_3)_2COH^+$	217
$CH_2COH^+OCH_3$ (*m/z* 74)	NA
$CH_2CHCOH^+OCH_3$ (*m/z* 87)	NA

that the amount of fragmentation increased as the alkyl chain length became shorter. This is not unusual. During ionization a certain amount of energy (0 to ~10 eV) is deposited into the molecular ion, which can result in its fragmentation. The longer the alkyl chain, the greater is the number of vibrational modes with which the excess internal energy can be redistributed, thus reducing the probability of fragmentation. Along with differences in fragmentation, Tulloch and Hogge[8] observed a significant increase in M_1^+ as the alkyl chain became shorter. They concluded that the instability of the molecular ion and the increase in M_1^+ were common to shorter alkyl chains. Fagerquist and Hellerstein[24] recently repeated a similar experiment with FAMES from methyl decanoate to methyl stearate on a Hewlett–Packard 6890/5972 quadrupole GC/MS system. A linear decline in $\sum_{m=0-2} I_m$/TIC was observed and an exponential increase in $I_{m=1}/I_{m=0}$ as the alkyl chain length became shorter. These results strongly suggest that fragment ions are responsible for the observed increase in $I_{m=1}/I_{m=0}$, and that proton transfer is the most likely mechanism based on thermochemistry and relative ion populations.

We are, to some extent, simplifying the issues involved. Proton transfer, hydride ion abstraction and hydrogen abstraction will also have an associated activation barrier. Proton transfer is likely to have the smallest activation barrier because no formal bonds are broken. The proton is simply exchanged between the electron lone pairs of the carbonyl oxygens of the cation and neutral. In contrast, hydrogen and hydride ion abstraction would require the breaking of a C—H bond first. The transition state for an abstraction process would have a non-negligible activation barrier and, in consequence, decrease the rate of abstraction.

It is important to point out that although proton transfer increases the mass of an ionized neutral molecule by 1 Da and hydride ion abstraction decreases the mass of the ionized neutral molecule by 1 Da, the combined effect of these two mechanisms on MIARs does not cancel out even if the amounts of proton donation and hydride ion abstraction are identical. For instance, methyl palmitate with natural abundance has a normalized abundance of $M_0 = 0.8229$, $M_1 = 0.1592$ and $M_2 = 0.0179$. If we assume 1.0% proton donation and 1.0% hydride ion abstraction, then $M_0 = 0.8229 - (2 \times 0.008\,229) + (0.001\,592)$, $M_1 = 0.1592 - (2 \times 0.001\,592) + 0.008\,229 + 0.000\,179$ and $M_2 = 0.0179 - (2 \times 0.000\,179) + 0.001\,592$. The new abundances are then $M_0 = 0.8080$, $M_1 = 0.1644$ and $M_2 = 0.019\,13$. Normalization gives $M_0 = 0.8149$, $M_1 = 0.1658$ and $M_2 = 0.0193$. Thus, we find that even equal amounts of proton donation and hydride ion abstraction will cause overestimation of the less abundant isotopomers and underestimation of the most abundant isotopomer.

The preceding discussion leads to another important point: the extent to which self-CI reactions affect the MIARs is, to a large extent, dependent on the number of molecules which are ionized by EI (but do not fragment) *vs.* the number of molecules which are ionized by self-CI (and do not fragment). Molecular ions generated by EI but which subsequently dissociate increases the relative proportion of molecular ions generated by self-CI while concomitantly creating more fragment ions for self-CI reactions. It should also be noted that ionization by self-CI should cause little, if any, fragmentation because of its small exothermicity (proton transfer) or endothermicity (hydride ion abstraction), thus increasing the relative population of self-CI molecular ions compared with EI molecular ions. In the previous hypothetical discussion, 98.0% of the molecular ions originated from EI ionization, whereas 2% originated from self-CI (equal amounts of proton donation and hydride ion abstraction), and yet this relatively small percentage of self-CI resulted in significant changes in the MIARs from the standpoint of mass isotopomer abundance measurements.

The mass analyzer

Carrier gas pressure. The possibility of ion scattering by ion–ion repulsions and ion–neutral collisions in the mass analyzer can potentially cause significant problems for accurate and precise isotopic measurements on sector-field instruments. The direction and velocity focusing of an E/B sector-field instrument should compensate for ion scattering caused by ion–neutral collisions in the source. However, ion scattering by ion–neutral collisions which occur after the main exit slit of the source can lead to peak broadening and overlap of adjacent isotopomers, i.e. tailing. Tailing of adjacent isotopomers will lead to underestimation of the most abundant isotopomer and overestimation of the less abundant isotopomers. The phenomenon is referred to as abundance sensitivity.[12] An obvious remedy is to reduce the pressure in the mass analyzer. Walder and Freedman[3] achieved an analyzer base pressure of 2.7×10^{-9} Torr using four stages of differential pumping on an ICP-MS E/B sector-field instrument to obtain accurate isotopic abundance measurements of metallic ions.

In order to test the effect of analyzer pressure on our isotopomer measurements, we varied the flow rate of the carrier gas from the GC capillary into the source. Source pressure was monitored by a Penning ion gauge located above the 6 in diffusion pump of the source. The analyzer pressure was monitored by the Penning ion gauge located above the 3 in diffusion pump which is attached to the electric-sector of the analyzer via a 90° elbow. Our initial experiments involved using helium, which is the most widely used carrier gas for gas chromatography. Within experimental error, we observed no significant change in MIARs at the two different source pressures: $<1 \times 10^{-6}$ and 2.5×10^{-6} Torr (with corresponding GC head pressures of 2.0 and 20.0 psi, respectively). Attempts to use even higher pressures automatically closed the source gate valve.

We repeated the same experiment using argon as a carrier gas, with the expectation that its greater mass of $M_r = 40$ compared 4 for helium would be more effective at ion scattering during an ion–molecule collision. As noted in the Results section, we observed a significant change in MIARs as a function of the argon pressure as shown in Fig. 3. We observe a decrease in M_0 and an increase in M_1 as the argon pressure in the source increased from 7×10^{-6} to 1.5×10^{-5} Torr (as measured by the Penning ion gauge of the source). M_2 was

actually found to decrease somewhat at the higher argon pressure. However, since TIIA was also found to decline at higher pressures (probably owing to the sample molecules being swept from ionization housing faster), it may be that the decline M_2 was the result of $I_{m=2}$ disproportionately falling within the signal-to-noise ratio level of the detector and insufficient compensatory gain from $I_{m=1}$ overlap with $I_{m=2}$ due to peak broadening.

Carboxylate anion of palmitate. Pentafluorylbenzyl palmitate was ionized by ECNCI to give the fragment carboxylate anion of palmitic acid. Although ECNCI is not strictly chemical ionization, it does use a 'reagent' gas (methane) for the purpose of slowing electrons which increase the likelihood of their capture by the sample molecule.[20] The electron affinity (EA) of the sample molecule obviously plays a critical role in the electron-capture process (in addition to fragmentation). In consequence, fluorinated compounds are very effective for ECNCI because of their high EAs.

The most striking result in Fig. 6 is the change in MIARs with the change in methane pressure. We see a significant drop in M_0 and increase in M_1 and M_2 for all samples sizes at the higher methane pressure. TIIA does not change significantly with pressure if the same amount of material is injected. The slight drop in TIIA at the higher pressure is probably due to greater ion scattering by methane molecules; however, the drop in TIIA is not sufficient to explain the significant changes in MIARs as due to detector non-linearities or ion–ion repulsions in the mass analyzer.

It is possible that the change in MIARs at the higher pressure may be due to gas-phase chemistry occurring in the source, such as hydrogen addition. However, after examining this possibility, we could not arrive at any plausible reaction mechanism which seemed kinetically or thermodynamically favorable. Ion–methane collisions in the source would cause negligible peak broadening due to velocity and direction convergence of double-focusing mass spectrometers. In consequence, we concluded that the decline in M_0 and increase in M_1 and M_2 at the higher methane pressure are due to ion–methane collisions in the analyzer which lead to peak broadening and 'tailing' of the more abundant isotopomer(s) overlapping with the less abundant isotopomers. In consequence, the less abundant isotopomers are overestimated and the more (or most) abundant isotopomer is underestimated.

The detector

As shown in Fig. 4, we observe a significant change in MIARs and increase in TIIA as a function of increasing electron multiplier voltage (EMV). The fact that M_2, the least abundant isotopomer, increases with increasing EMV may suggest that a disproportionate amount of $I_{m=2}$ falls within the signal-to-noise ratio level of the detector–amplifier system which would result in underestimation of M_2 at lower EMV. Bergner and Lee,[13] using a Hewlett-Packard 5890/5971 quadrupole GC/MS system, noted the effect of linear *vs.* non-linear amplifying circuit boards on the relative isotopic abundances of labeled glucose. They emphasized the importance of using linear boards for quantitative isotopomer abundance measurements. The amplifying circuit board on the AX505 is linear, but the 16-dynode cascade electron multiplier has a non-linear response (as is the case for all electron multipliers). Hence the entire detector–amplifier system has a non-linear response.

It is obvious that detector non-linearities can have a significant effect on MIARs. We have noted before that the y-intercept for $I_{m=1}/I_{m=0}$ *vs.* $I_{m=0}$ in Fig. 2 and that for $I_{m=2}/I_{m=1}$ *vs.* $I_{m=1}$ in Fig. 3 are below their correct natural abundance values. It is possible that underestimation of the y-intercept is due to the less abundant isotopomer falling disproportionately within the signal-to-noise ratio level of the electron multiplier (which becomes increasingly severe as the sample size decreases). In other words, as the sample size decreases, gas-phase chemistry decreases with the square of the sample size, but detector non-linearities increase. Hence, for small sample sizes, inaccuracies in MIARs are due primarily to detector non-linearity. It is interesting that the y-intercept for $I_{m=1}/I_{m=0}$ *vs.* $I_{m=0}$ reported by Patterson and Wolfe[9] was even more underestimated than our value; however, since it is well known that electron multiplier sensitivity diminishes with time, this may reflect nothing more than differences in electron multiplier gain between the two instruments.

CONCLUSIONS

Our results on the mass isotopomer measurements of methyl palmitate by GC/EI-MS on a sector-field double-focusing mass spectrometer lead us to conclude that the concentration dependence is a reflection of two off-setting factors: (i) gas-phase chemistry in the source, specifically proton transfer between fragment cations and neutral molecules and (ii) detector non-linearities, specifically the underestimation of less abundant isotopomers due to their signal disproportionately falling within the signal-to-noise ratio level of the electron multiplier detector. Gas-phase chemistry is the dominant cause of inaccuracy in MIAR measurements for large sample sizes, whereas detector non-linearity is the dominant cause of inaccuracy in MIAR measurements at low sample sizes (where very little gas-phase chemistry occurs). However, in a narrow range of sample sizes, these two compensatory effects balance each other, resulting in 'correct' MIARs (for compounds whose isotopic composition is known). However, caution must be exercised for the analysis of samples containing compounds of unknown isotopic enrichment since the concentration range which is 'acceptable' for a compound of known isotopic composition also reflects the detector's response to the MIARs of the known (which is likely to be different from the unknown). We would also emphasize that these two effects are present regardless of the type of mass analyzer used: quadrupole, sector-field, etc. Improvements in accuracy and precision of mass isotopomer abundance measurements, by advances in mass spectrometric design, would therefore need to eliminate each cause of inaccuracy. For example, a more 'open' type of source, designed exclu-

sively for EI, might reduce the amount of self-CI reactions.

Finally, our results suggest that ion scattering by ion–neutral collisions in the mass analyzer do not play a significant role in the concentration effect for methyl palmitate by GC/EI-MS. However, for high-pressure ionization techniques, such as CI, where the pressure in the mass analyzer may be significantly higher, ion–neutral collisions may play a significant role in MIARs, as reflected in our results using argon as a GC carrier gas and our pressure-dependent results with ECNCI.

Acknowledgements

This research was supported by a grant of the Bay Area Nutrition Center and the Agricultural Experimental Station projects and USDA competitive and special grant. We thank Dr Robert B. Cody, Mr Shin'ichi Miki and Dr Kenny Caldwell for stimulating discussions. We acknowledge JEOL for the normal-scan spectrum of methyl palmitate. We also thank Professor B. Munson and Dr J. A. Evans for allowing us to cite their unpublished gas-phase basicity measurements.

REFERENCES

1. K. J. Goodman and J. T. Brenna, *J. Chromatogr. A* **689**, 63 (1995).
2. J. T. Brenna, *Acc. Chem. Res.* **27**, 340 (1994).
3. A. J. Walder and P. A. Freedman, *J. Anal. At. Spectrom.* **7**, 571 (1992).
4. (a) M. K. Hellerstein, M. Christiansen, S. Kaempfer, C. Kletke, K. Wu, J. S. Reid, K. Mulligan, N. S. Hellerstein and C. H. Shackleton, *J. Clin. Invest.* **87**, 1841 (1991); (b) M. K. Hellerstein, *J. Biol. Chem.* **266**, 10920 (1991); (c) J. Katz and W. N. Lee, *Am. J. Physiol.* **261**, E332 (1991); (d) J. K. Kelleher and T. M. Masterson, *Am. J. Physiol.* **262**, E118 (1992); (e) M. K. Hellerstein and R. A. Neese, *Am. J. Physiol.* **263**, E988 (1992).
5. (a) W. N. Lee, E. A. Bergner and Z. K. Guo, *Biol. Mass Spectrom.* **21**, 114 (1992); (b) W. N. Lee, L. O. Byerley, E. A. Bergner and J. Edmond, *Biol. Mass Spectrom.* **20**, 451 (1991); (c) W. N. Lee, S. Sorou and E. A. Bergner, *Biochem. Med. Metab. Biol.* **45**, 298 (1991).
6. (a) S. F. Previs, C. Des Rosiers, M. Beylot, F. David and H. Brunengraber, *J. Mass Spectrom.* **31**, 643 (1996); (b) C. A. Fernandez, C. Des Rosiers, S. F. Previs, F. David and H. Brunengraber, *J. Mass Spectrom.* **31**, 255 (1996); (c) S. F. Previs, C. A. Fernandez, D. Yang, M. V. Soloviev, F. David and H. Brunengraber, *J. Biol. Chem.* **270**, 19806 (1995); (d) B. R. Landau, C. A. Fernandez, S. F. Previs, K. Ekberg, V. Chandramouli, J. Wahren, S. C. Kalhan and H. Brunengraber, *Am. J. Physiol.* **269**, E18 (1995); (e) C. Des Rosiers, L. Di Donato, B. Comte, A. Laplante, C. Marcoux, F. David, C. A. Fernandez and H. Brunengraber, *J. Biol. Chem.* **270**, 10027 (1995); (f) M. Beylot, S. F. Previs, F. David and H. Brunengraber, *Anal. Biochem.* **212**, 526 (1993).
7. (a) H. Brunengraber, J. K. Kelleher and C. Des Rosiers, *Annu. Rev. Nutr.* **17**, 559 (1997); (b) M. K. Hellerstein, *Lipids* **31**, S117 (1996); (c) T. M. Masterson and J. K. Kelleher, *Comp. Biol. Med.* **26**, 429 (1996); (d) M. K. Hellerstein, J.-M. Schwarz and R. A. Neese, *Annu. Rev. Nutr.* **16**, 523 (1996); (e) M. K. Hellerstein, *Curr. Opin. Lipids* **6**, 172 (1995); (f) J. Katz, P. Wals and W. N. Lee, *J. Biol. Chem.* **268**, 25509 (1993).
8. A. P. Tulloch and L. R. Hogge, *Chem. Phys. Lipids* **37**, 271 (1985).
9. B. W. Patterson and R. R. Wolfe, *Biol. Mass Spectrom.* **22**, 481 (1993).
10. M. G. Kienle and F. Magni, *Biol. Mass Spectrom.* **23**, 173 (1994).
11. J. Zamecnik, C. Fayolle and A. Vallerand, *Biol. Mass Spectrom.* **23**, 804 (1994).
12. (a) P. Deines, *Int. J. Mass Spectrom. Ion Phys.* **4**, 283 (1970); (b) S. J. Prosser, *Int. J. Mass Spectrom. Ion Processes* **125**, 241 (1993); (c) S. J. Prosser and C. M. Scrimgeour, *Anal. Chem.* **67**, 1992 (1995); (d). J. J. Stoffel and H.-J. Laue, *Int. J. Mass Spectrom. Ion Processes* **105**, 225 (1991); (e) J. J. Stoffel, D. R. Ells, L. A. Bond, P. A. Freedman, B. N. Tattersall and C. R. Lagergren, *Int. J. Mass Spectrom. Ion Processes* **132**, 217 (1994).
13. E. A. Bergner and P. W.-N. Lee, *J. Mass Spectrom.* **30**, 778 (1995).
14. F. W. McLafferty, *Anal. Chem.* **82**, 31 (1959).
15. Ng Dinh-Nguyen, R. Ryhage, S. Stallberg-Stenhagen and E. Stenhagen, *Ark. Kemi* **18**, 393 (1961).
16. M. Takayama, *Int. J. Mass Spectrom. Ion Processes* **144**, 199 (1995).
17. H. D. Beckey, H. Hey, K. Levson and G. Tenschert, *Int. J. Mass Spectrom. Ion Processes* **2**, 101 (1969).
18. H. D. Beckey, *Int. J. Mass Spectrom. Ion Processes* **1**, 93 (1968).
19. C. W. Tsang and A. G. Harrison, *J. Chem. Soc., Perkin Trans. 2* **2**, 1718 (1975).
20. A. G. Harrison, *Chemical Ionization Mass Spectrometry*, 2nd edn. CRC Press, Boca Raton, FL (1992).
21. J. A. Evans, B. Munson, G. Nicol and R. Tosh, ASMS June 1997.
22. D. H. Aue, M. T. Bowers, in *Gas Phase Ion Chemistry*, edited by M. T. Bowers, Vol. 2, pp 1–51. Academic Press, New York (1979).
23. S. G. Lias, J. E. Bartmess, J. F. Liebman, J. L. Holmes, R. D. Levin and W. G. Mallard, *J. Phys. Chem. Ref. Data* **17**, Suppl. 1, 24 (1988).
24. C. K. Fagerquist and M. K. Hellerstein, to be submitted.